SLIDING MODES IN INTERSECTING SWITCHING SURFACES, II: HYSTERESIS

JAMES C. ALEXANDER AND THOMAS I. SEIDMAN

ABSTRACT. When a flow, discontinuous across a switching surface, points "inward" so one cannot leave, it induces a unique flow within the surface, called the *sliding mode*. Uniqueness of sliding modes does not obtain in general when several such surfaces intersect, and models must be refined. Following our earlier papers, we investigate the consequences of such refinements. We show that a natural mechanism, to wit *hysteresis*, which has been extensively investigated for one switching surface, generically leads to a well-defined sliding mode in the intersection of two switching surfaces.

1. INTRODUCTION

In previous papers [**5**], [**1**], the authors considered issues concerned with the dynamics of differential systems

$$\dot{x} = f(x), \tag{1.1}$$

on d-dimensional state space near certain surfaces $\mathcal{S}_j$ of f; the vector field f is uniformly Lipschitz except for permitted jump discontinuities, which may be viewed as a switching of "modes," across certain smooth codimension-1 manifolds $\mathcal{S}_j$, termed *switching surfaces.* Continuing the lines of investigation of [**5**], [**1**], we wish to explain the (otherwise indeterminate) local behavior at the intersection of more than one $\mathcal{S}_j$.

We consider particularly the situation that the vector fields f point "inward" with non-zero speed towards any $\mathcal{S}_j$ (the inner product of the field near the surface and a normal pointing outward from $\mathcal{S}_j$ is uniformly negative). The flow of (1.1) in a neighborhood of a surface reaches the surface in finite time and is then trapped there. The issue is to develop a well-defined concept of the subsequent behavior of the flow "along" the switching surface, the *sliding mode.* In particular, the vector field defining the sliding mode is tangent to the switching surface at all

Received by the editors March 13, 1998.

such points. If there are several such surfaces that intersect, the flow becomes trapped in the intersection, and the issue is the same.

The local behavior in the case of one switching surface $\mathcal{S}$, extensively analyzed in [**3**], is well understood and has an essentially unique answer. One can think of $\mathcal{S}$ as the 0-manifold of a smooth *sensor functional*. Filippov imposed a condition, termed the *Filippov condition* in [**1**]; that, at each point of the switching surface, the vector defining the sliding mode is both tangent to $\mathcal{S}$ and a convex combination of the impinging fields. He noted that this condition is sufficient to guarantee uniqueness of the sliding mode. Intersecting surfaces can be considered the 0-manifolds of several sensor functionals. The corresponding Filippov condition is generally insufficient to determine a sliding mode and more refined assumptions must go into the analysis. Indeed, in [**1**], it is shown that the number of degrees of freedom in the lack of uniqueness generically goes up exponentially in the number of intersecting surfaces. In any particular model, these refined assumptions come from the application being modelled; we call them the *mechanism* of the model, related to the nature of a physical implementation of (1.1).

The authors have considered one mechanism [**1**], termed *blending*, in which the switching of modes is not instantaneous across an $\mathcal{S}_j$, but rather occurs continuously in a region (boundary layer) of width 2ϵ near the $\mathcal{S}_j$ (see e.g., the example of simple friction in [**6**, pages 1-3]). For the case of two intersecting surfaces $\mathcal{S}_1$ and $\mathcal{S}_2$, we showed that blending, together with the Filippov condition, led to a unique well-defined vector at each point of $\mathcal{S}_1 \cap \mathcal{S}_2$, by which the sliding mode is defined.

In the present paper, we consider the issue for a different mechanism, *hysteresis*, which has been developed extensively for one switching surface [**3**]. With hysteresis, the switch from one mode to another does not occur at the switching surface, but rather after the trajectory has travelled a farther distance of ϵ. Thus a trajectory "chatters" back and forth across the switching surface. It is assumed ϵ is small so the chattering is rapid compared to the natural scale of the flow; that is, the problem has multiple scales. The average of the impinging vector fields, weighted by the proportions of time the flow spends in each mode, if well-defined, is the field of the sliding mode. Calculation shows it is then tangent to the switching surface and is thus indeed a sliding mode; by construction, it satisfies the Filippov condition. Here we consider the case of two intersecting hysteretic switching surfaces and show that generically (in a sense made precise below) the mechanism leads to a well-defined sliding mode. The analysis uses the general theory (which goes back to Poincaré) of flows of doubly-periodic vector fields, along with some structure particular to the situation at hand. The results are not as clear cut as for blending, in that the result is only generic, and this leads to some delicate questions for future consideration; see Section 8.

2. Hysteresis

In this section, we make precise the mechanism of hysteresis, and, following [**5**], set up the framework for our analysis. In [**1**], we discussed transversality, normal positioning and scaling of switching surfaces, and we assume the results of that discussion here. We restrict our attention to two intersecting switching surfaces. Our results are local, so we may assume our state space is Euclidean. We also suppose that the speeds of approach to the two switching surfaces are "commensurate." That is, neither is asymptotically "infinitely fast" compared to the other, in which case, the analysis would reduce to an easier analysis [**3**]. Thus we assume given a differential system (1.1) defined on $R^2 \times R^{d-2}$ (thus emphasizing the first two coordinates). In R^2, let $Q_1, \ldots, Q_4$ denote the four open quadrants, and let $X = \{(x,y) : y = 0\}$ and $Y = \{(x,y) : x = 0\}$ be the coordinate lines. The hyperplanes $X \times R^{d-2}$ and $Y \times R^{d-2}$ are the *switching surfaces*, and of course they intersect along $\{0\} \times R^{d-2}$. We assume f of (1.1) is Lipschitz, except on $(X \cup Y) \times R^{d-2}$.

Since with hysteresis there is a delay of switching after the trajectory crosses the switching surface, we must be more precise. Thus, suppose f_i are defined and Lipschitz on a neighborhood of $\overline{Q}_i \times R^{d-2}$ and that $f = f_i$ on $\overline{Q}_i \times R^{d-2}$. For any point $z \in R^{d-2}$, identify R^2 with $R^2 \times \{z\}$. If $f_i(x,y,z)$ has components $\big(v_i(x,y,z), w_i(x,y,z)\big)$ in $R^2 \times R^{d-2}$, we suppose each $v_i(x,y,z)$ "points inward." More precisely, let $\hat{\imath}_i$ and $\hat{\jmath}_i$ be the unit vectors in the x and y directions in Q_i, pointing *into* $Q_i \subset R^2 \times R^{d-2}$ (that is, $\hat{\imath}_i$ has positive (respectively negative) x component for $i = 1$, 4 (respectively $i = 2$,3) and $\hat{\jmath}_i$ has positive (respectively negative y) component for $i = 1$, 2 (respectively $i = 3$, 4)). Pointing inward means the dot products $v_i(x,y,z) \cdot \hat{\imath}_i < 0$ and $v_i(x,y,z) \cdot \hat{\jmath}_i < 0$. It is clearly sufficient that $v_i(0,0,z) \cdot \hat{\imath}_i < 0$ and $v_i(0,0,z) \cdot \hat{\jmath}_i < 0$. See Figure 2.

Let $\epsilon \ll 1$. Define

$$B = B_\epsilon = \{(x,y) : |x| \le \epsilon, |y| \le \epsilon\} \subset R^2, \tag{2.1}$$

a "box" of side 2ϵ. We call either B or $B \times R^{d-2}$ the *chatterbox*. We suppose that ϵ is small enough that we can suppose B is a boundary layer; i.e., that effectively $\epsilon \to 0$. In particular, we suppose ϵ is small enough that all f_i are defined throughout B.

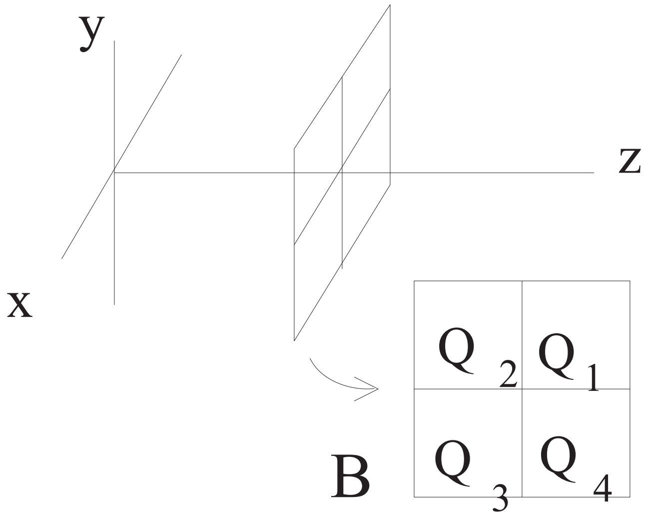

FIGURE 1. The transversal chatterbox B. Our analysis proceeds on the two-dimensional box for fixed (frozen) z. The quadrants $Q_1, \ldots, Q_4$ are indicated.

We next define the hysteretic flow. We give a descriptive definition, leaving the interested reader to develop formulae; compare [**5**] and [**3**]. At each point, a trajectory $T = T(t)$ has its value in the state space, obeying one of the differential equations

$$\dot{x} = f_i(x), \tag{2.2}$$

indexed by the quadrant. At any t, if the trajectory obeys (2.2) with index i, we say the trajectory is in *mode* i. The trajectory "senses" when it crosses X or Y, but does not "act" on this knowledge until distance ϵ later. Horizontal and vertical indices (m_h, m_v) store the crossing information. Obeying (2.2), a trajectory $T = T(t)$ enters some $(B \cap Q_i) \times R^{d-2}$ in finite time, where we begin monitoring T. The mode and the horizontal and vertical indices are set as follows: whenever $T(t)$

(a). crosses $X \times R^{d-2}$ from Q_i to Q_j, m_h is set to j,
(b). crosses $Y \times R^{d-2}$ from Q_i to Q_j, m_v is set to j,
(c). hits a boundary ("wall") of B at $\{|x| = \epsilon\}$, the mode is changed to m_h,
(d). hits a boundary ("wall") of B at $\{|y| = \epsilon\}$, the mode is changed to m_v.

The trajectory "bounces" off of the edge of B and returns to the interior of B. There are also limiting degenerate cases when $T(t)$ crosses $X \cap Y = \{0\}$, or hits a corner of B. Conventions can be set for these cases; however since they occur for a set of initial conditions of measure zero and do not affect our analysis, we do not concern ourselves with these. However, we note that these "corner" cases become exactly the critical situations (from a different point of view) in §5. The issue is that the trajectory continuation is continuous across such an event. We also note that the trajectory, as a set, is entirely determined by the driections of the vectors f_i although the associated time fractions necessarily depend on their magnitudes, which give the speeds.

We have supposed $\epsilon \ll 1$. Then the chattering occurs rapidly compared to the natural time scale of the components of the trajectory in the R^{d-2} directions. We suppose it sufficiently small that it is reasonable to consider two time scales, the chattering scale and the other, the *natural* scale, of the fields (mathematically, we let $\epsilon \to 0$). We suppose z is quasi-stationary, and consider the chattering dynamics; i.e., the dynamics of the x and y components of (2.2) for fixed z. We say that z is *frozen*; see Figure 1. For each z, we wish to use the chattering dynamics to define a vector $g(z)$, which is to be the governing vector field for the *sliding mode*; that is, the sliding mode of z should obey a differential equation

$$\dot{z} = g(z). \tag{2.3}$$

Stated in this generality, $g(z)$ is a vector in R^d. To generate a sliding mode, it must be tangent to the switching surface R^{d-2}; this requires proof.

Suppose there is a long-term average dynamic behavior of T in the chatterbox so that, *independent of the initial condition of* T, the proportion of time spent in mode i is asymptotically $c_i = c_i^\epsilon(z)$, where

$$c_i^\epsilon(z) \geq 0, \qquad \sum_i c_i^\epsilon(z) = 1. \tag{2.4}$$

Then, following Filippov [**3**], $g(z)$ is the weighted average of the $f_i(0, 0, z)$;

$$g^\epsilon(z) = \sum_i c_i^\epsilon(z) f_i(0, 0, z). \tag{2.5}$$

The weights c_i^ϵ are termed the *Filippov coefficients*. It is precisely the existence of such behavior for dynamical systems of this special form that is our principal concern in this paper.

Suppose, ignoring where the weights might come from, one considers weighted sums (2.6) satisfying (2.4) (where for the nonce we consider N intersecting surfaces, not only $N = 2$), and considers whether the Filippov coefficients of (2.6) are uniquely defined for each z by the requirement that $g(z)$ be tangent to the switching surfaces. For one switching surface, the Filippov condition is sufficient to specify the Filippov coefficients (2.6) of a sliding mode uniquely [**3**]. However, for N intersecting switching surfaces, the Filippov condition is not sufficient and the set of possible Filippov coefficients is a compact convex set of dimension $2^N - N - 1$ [**1**], so in particular for $N = 2$, there is a line segment of such coefficients.

One approach to the indeterminancy is to consider $g(z)$ a set-valued function, and proceed in that vein. Another is to supplement the tangency requirement by additional conditions. These conditions come from refinements of the model underlying the analysis and are termed *mechanisms*; see [**1**], where one mechanism, sigmoid blending, was considered that leads to unique Filippov coefficients. Here we consider the implications of the mechanism of *hysteresis*.

The question of uniqueness is a pointwise issue in z. Accordingly, we fix z and drop it from the notation. Moreover, this question depends only on the components v_i of the f_i in R^2, and we restrict attention to these components, and develop answers to our questions in terms of the v_i and the resulting dynamics in the chatterbox B in R^2, which we call the *chattering dynamics*.

We expand on our use of the fact that $\epsilon \ll 1$. For such ϵ each of the vector fields $f_i(x, y, z)$ is a small perturbation of its limit $f_i(0, 0, z)$, and as $\epsilon \to 0$, can be replaced by its limit. It is technically (and notationally) more convenient to work with the dynamical system defined by these limiting vectors, i.e., where each $f_i(x, y, z) = f_i(0, 0, z)$ is constant in x and y. Thus we consider the chattering dynamics of the system defined by four constant vectors $f_i(0, 0, z)$, with the corresponding Filippov coefficients $c_i = c_i^0(z)$ and sum

$$g(z) = g^0(z) = \sum_i c_i(z) f_i(0, 0, z). \tag{2.6}$$

This raises the issue of the relation between $g^\epsilon(z)$ and $g(z)$, and whether the dynamics of the limiting system captures the limit of the dynamics of the ϵ system as $\epsilon \to 0$; this is the content of Theorem 2.3 below.

Consider the set of vector fields on R^2, constant on each quadrant, equivalently the set of four vectors. This set is parametrized by R^8 (two components for the vector in each quadrant). The inward-pointing vector fields Φ form an open subset. We cannot show existence/uniqueness of a sliding mode for every quadruple in Φ (see Section 8), but as our principal result, we do prove the following result.

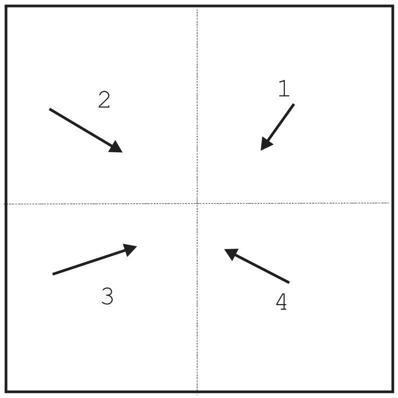

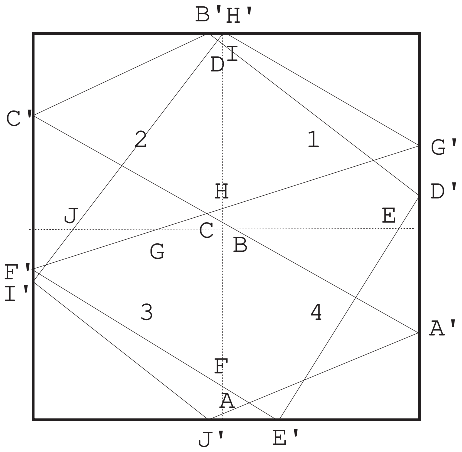

FIGURE 2. The left figure illustrates a chatterbox with four different vectors in the four quadrants, all pointing "inward." The right figure illustrates a periodic chattering trajectory in this chatterbox. Although the trajectory crosses, e.g. from quadrant 3 to quadrant 4 at A, the trajectory does not "react" until it hits the "wall" at A'. Similarly for B through J. Note that the crossing of the horizontal surface at B occurs before the crossing of the vertical surface at C on the trajectory, but C' occurs before B', since B is a horizontal crossing and C is a vertical one.

Theorem 2.1. *For an open dense subset Φ' of vector fields in Φ, the chattering dynamics in R^2 has a single stable attracting periodic trajectory P.*

An open dense subset such as Φ' is called *generic*. The point of Theorem 2.1 is that for a vector field in Φ', all trajectories but one (a single unstable periodic trajectory P') tend asymptotically to this attracting periodic trajectory P in the chattering dynamics. For a periodic trajectory, there is certainly an average long-time behavior (repetition), and the Filippov coefficients c_i are thus defined. Almost all trajectories have the same asymptotic behavior, and the Filippov coefficients adequately capture the long-term dynamic behavior. That is, each coefficient $c_i(z)$ is the asymptotic fraction of time spent in mode i for an almost arbitrary trajectory corresponding to the dynamics of the frozen fields. Moreover, the Filippov sum (2.6) defines a sliding mode by the following.

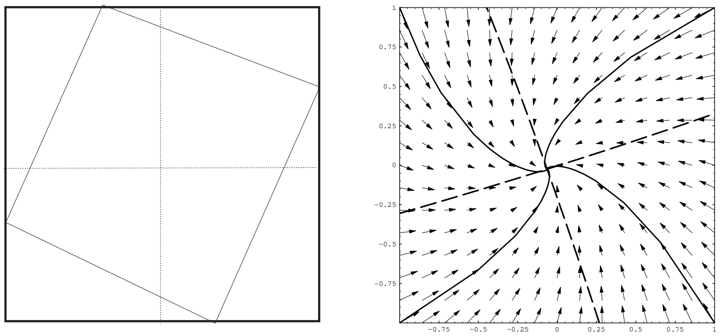

FIGURE 3. Left: A stable trajectory for the hysteretic model given in Table 1. The trajectory evolves clockwise. Right: The blending dynamics. To understand the particulars of the figure, the reader is referred to [**1**]. However, all that we need note here is that the proportions in Table 1 are determined by the coordinates of the stationary point of the vector field, at the point where the lines cross and the trajectories terminate. This point is in the third quadrant, and we note the weight for the third quadrant given in Table 1 is largest.

Theorem 2.2. *For vector fields in Φ', the Filippov sum (2.6) defined above is a sliding mode; that is $g(z) = \sum_i c_i(z) f_i(0,0,z) \in R^{d-2}$.*

Theorem 2.3. *For vector fields in Φ',*

$$\lim_{\epsilon \to 0} c_i^\epsilon(z) \to c_i^0(z) = c_i(z) \tag{2.7}$$

and the c_i depend locally Lipschitz on the fields, analytically on the fields in each component of Phi'.

These theorems are as good as can be expected. As can be seen by the proof (and by example), there are vector fields for which there is no single asymptotic behavior of its trajectories. However, although such fields occur for a null set of fields, as the system (2.6) evolves the chattering fields $v_i(z)$ vary and such fields are encountered. This raises further questions; see Section 8. We also note that the result of Theorem 2.1 is robust in the following sense. Since Φ' is open, small modifications to a field in Φ' do not change the qualitative behavior. In particular, if the shape of the chatterbox is changed slightly, the result still holds, and the system (2.3) has a smooth local solution within the intersection of the $\mathcal{S}_i$.

Developing the context and machinery to prove Theorem 2.1 is the main content of the paper. The proof of Theorem 2.1 consumes Sections 2–6. The proofs of Theorems 2.2, 2.3 follow in Section 7. Section 8 is a discussion section.

The chattering behavior is illustrated in Figure 2. Here a set of inward-pointing vectors in a chatterbox in R^2 is illustrated, with a resulting chattering trajectory.

Hysteresis and blending each lead to sliding modes, but we note these are generally different. That is, the Filippov coefficients c_i determining the sliding mode are different. For an explicit example, see Table 1 and Figure 3. Thus the specific physical assumptions, through "supplementary conditions" as noted above, are important to the appropriate resolution of the ambiguity otherwise inherent in the situation; there is no universal selection criterion.

Quadrant	Slope	Chatterbox weight	Blended weight
1	$3(1+\sqrt{3})/4 = -2.050$	.240	.228
2	$-(3+\sqrt{3})/(6+4\sqrt{3}) = .366$	.276	.260
3	$\sqrt{3} = 1.732$	.242	.272
4	$-\sqrt{3}/3 = -.577$	.242	.240

TABLE 1. Comparison of chatterbox and blending mechanisms. With the slopes of four unit vectors indicated in each of the four quadrants, the resulting proportions for the blending mechanism and hysteresis are indicated. These proportions are the weights for calculating the vector for the sliding mode; thus blending and hysteresis give different sliding modes.

3. Simulation

We report, in this section, on computer simulations of chattering dynamics. Figures 4, 5 are graphs of computer simulations of flows in tori, with several aspects of the flow indicated on each graph. For each of the four quadrants of the torus, a random angle is generated; this is the angle of the vector field. The four vectors of the field are normalized to common length. (Note: the norm does affect the dynamics and thus the coefficients c_i^ϵ, but does not affect the trajectories themselves, and thus does not affect the existence or not of a periodic orbit.) The random selection is done twice, and the fields are varied via linear interpolation with an interpolation parameter τ that varies from 0 (at the left) to 1 (at the

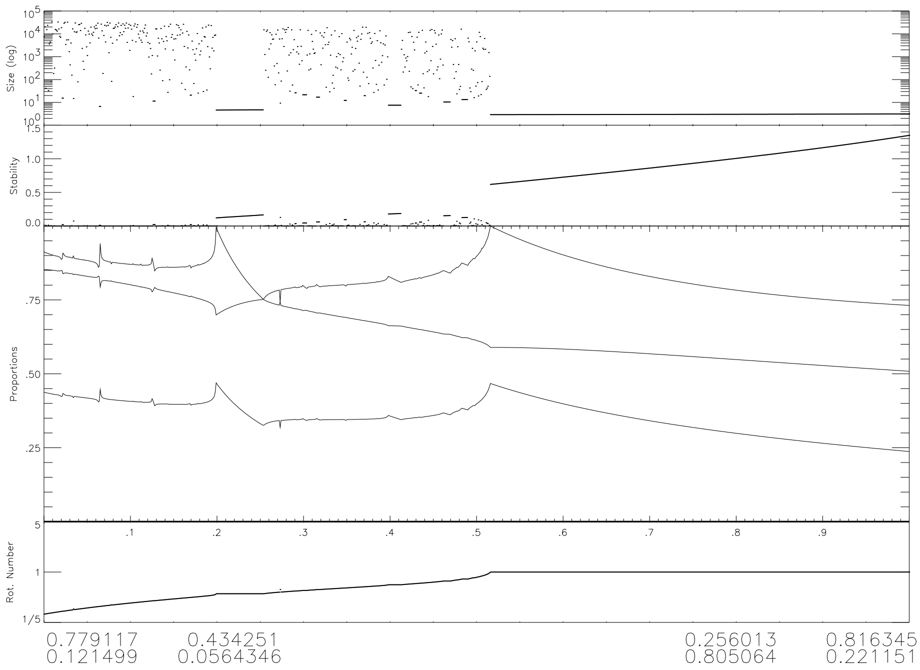

FIGURE 4. Plots of computer simulations of chatterbox dynamics. Two sets of random angles for the vectors in each of the four quadrants; the absolute values of these are indicated in the bottom left and right as proportions of $\pi/2$, listed by quadrant. One thousand linear interpolants of these two sets of angles were used; these interpolants span the horizontal axis. For each value of τ and resulting vectors, the system was integrated. A trajectory was calculated (in fact, since the system is piecewise constant, the trajectory was determined via a series of algebraic operations, not integration). The trajectory was "preiterated" 1000 times, so it could stabilize. Then it was run until it returned (within a threshold) to its initial value (hence is periodic) or for 10,000 loops around the torus. See also Figure 5.

right). The horizontal axis of each graph in Figures 4, 5 is τ; the angles of the four vectors at $\tau = 0$ and 1 (as multiples of $\pi/2$) are indicated at the bottom left and right of the graph. Computations are made for one thousand τ values along

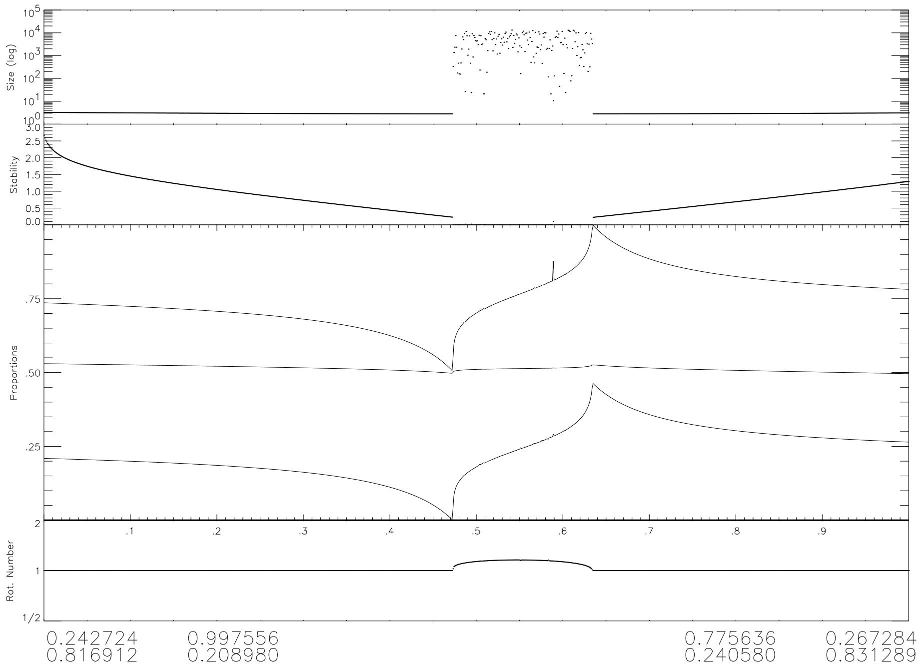

FIGURE 5. A second example of the plot of Figure 4. For these figures, four aspects of the flows are graphed. At the top, the length of the trajectory, scaled to ϵ, is plotted. Below that is the negative of the Floquet exponent (discussed below) per length is plotted. The larger this number, the larger this number, the more stable the trajectory. Below that, the proportions of time the trajectory spends in each of the four quadrants are indicated in a proportional chart; for each point on the horizontal axis, the proportions are indicated by the lengths of the four vertical segments, adding to 1. At the bottom, a rotation number (also discussed below) is calculated. The proportions, of course, are the Filippov coefficients c_i of (2.6).

the horizontal axis. At each τ value, the system is permitted to run for 1000 "preiterates" to effect stabilization; after that, the behavior of the trajectory is recorded, either until it returns to itself (a stable periodic trajectory), or until it crosses the horizontal coordinate of the torus 10,000 times. The top graph in each figure is the total length of the trajectory scaled by ϵ. Below that is the stability of the trajectory. This number is discussed in more detail in Section 5; however, the larger this number, the more stable the trajectory. Below that is a proportional chart of the time spent in each of the four quadrants—the heights between the lines, adding up to 1. Of course, these are the Filippov coefficients c_i of equation (2.6). Below that the rotation number is graphed. These simulations were initiated as part of a program to find multiple stable periodic trajectories, which the authors originally conjectured would occur. It was only after a number of simulations failed to turn up multiple stable trajectories that the authors sought to establish generic uniqueness.

The following behavior is indicated; it is explained analytically in the remainder of this paper: There are intervals of τ over which the rotation number is constant. The trajectory is periodic and clearly stable, and the Filippov coefficients c_i are clearly continuous in τ. In the underlying dynamics, there is one stable periodic trajectory and, as τ varies, the trace of this trajectory moves about the chatterbox continuously, never however, intersecting any of the corners of the torus, nor crossing the origin. At the ends of these τ intervals, the corresponding trajectory crosses one of the corners. It loses its stability and becomes neutrally stable. Near such τ values, there is rapid change of rotation numbers. For low rotation numbers, the length is relatively short and the stability is evident. The rotation number changes continuously in a so-called "devil's staircase" (intervals on which it is a constant rational, irrational on a set of measure zero). In these τ regions, there are very long orbits with marginal stability. We note the occurance of apparent jumps in the Filippov coefficients. However, these seem to disappear with more refined simulations, and they most likely are numerical effects of various threshholds set in the computer runs.

4. Doubly periodic vector fields

In this section, we begin the proof of Theorem 2.1. We recall some general existing theory of doubly-periodic vector fields and set our problem in this theory. In particular, we establish the generic existence of stable periodic orbits.

The first step, following [**5**], is to "unwind" the trajectory into a more manageable form. In geometric optics, dynamics of billiards, etc., where a trajectory "bounces," a useful technique is what is called in optics "virtual images." For our present analysis, it is not the situation that "the angle of reflection equals the angle of incidence," but the general philosophy works. When a trajectory hits,

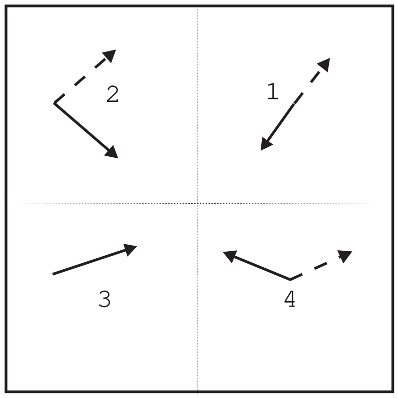

FIGURE 6. The vectors of Figure 2 flipped horizontally and/or vertically so they all point "northeast"—i.e., all components positive.

say, the right wall, instead of returning back into the chatterbox, it "refracts" onward to the right in this virtual image.

Recall that we replace the vector field in each quadrant with its value at the origin, and for convenience, we also rescale $\epsilon = 1$. The first technical step is to reorient the vectors so they all point up and to the right ("northeast"); see Figure 6. Thus the vector in Q_1 is replaced by its negative, the vector in Q_2 is reflected vertically, and the vector in Q_4 is reflected horizontally.

A trajectory refracts when it hits a wall of the chatterbox. The switching surfaces themselves thus lose their direct significance, and disappear from the dynamics. To completely capture the dynamics, we work with four copies (2×2 horizontal and vertical) of the chatterbox. These four copies are labelled (with slight abuse) also $Q_1, \ldots, Q_4$ and are assigned the corresponding relected vectors. We call the resulting figure a *fundamental domain* $\mathcal{F}$ of the dynamics. There are two standard constructions with fundamental domains. One is to identify opposite edges to form a torus. A trajectory that refracts through the right edge appears at the left after this identification. The second is to tile the plane with copies of $\mathcal{F}$. We label the copies $\mathcal{F}^{(m,n)}$ for pairs of integers (m,n) to indicate their coordinate position in the plane. Within $\mathcal{F}^{(m,n)}$ are copies $Q_1^{(m,n)}, \ldots, Q_4^{(m,n)}$. Moreover, the trajectory can be "unwound" through the tiling; see Figure 7, where six copies (3×2) of the fundamental domain are shown. Moreover, the orbit of Figure 2 is unwound in this figure. We call a collection of $m \times n$ fundamental domains, as

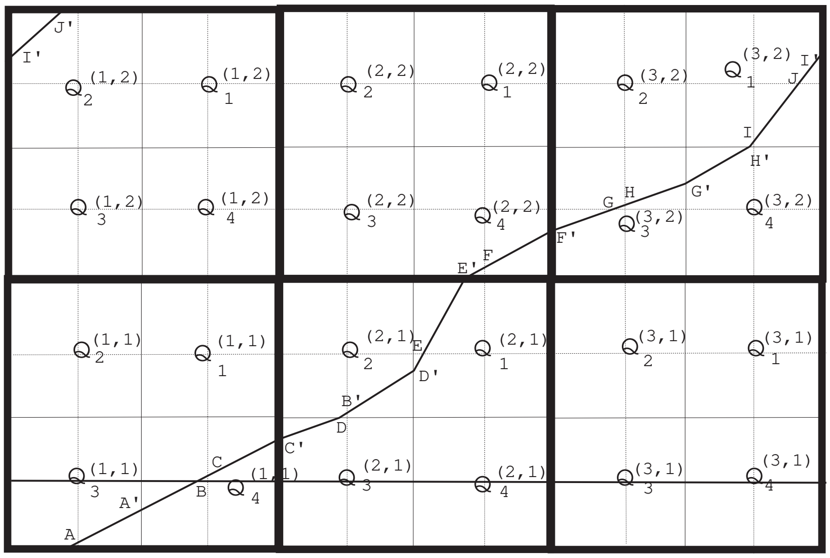

FIGURE 7. The resulting trajectory is considered a trajectory on the torus. This figure is rescaled from previous figures. A fundamental domain consists of four (two by two) copies of the domain of Figure 2 (or Figure 6). This figure consists of six (two by three) copies of the fundamental domain. In each fundamental domain, there are four different vector fields equal to the fields of the four quadrants of Figure 6. These four regions are the $Q_k^{(i,j)}$ indicated on the figure. In figures below, these regions are indicated only by their subscripts. This flow contains precisely the same information as the flow of Figure 2 (and indeed, by cutting and overlaying the fundamental domains on each other, and then folding, the trajectory of this figure be overlaid on the trajectory of Figure 2).

in Figure 7, an (m, n)-*fundamental domain.* If we identify opposite edges of an (m, n)-fundamental domain, we obtain a new torus, an (m, n)-*torus.* Note that (m, n)-fundamental domains are subsets of the plane, and (m, n)-tori are quotient spaces. Fundamental domains are easier to picture; tori are where the dynamics really occurs. In fact, note that the last bit of the trajectory in Figure 7 is actually shown in the upper left, as in a torus, rather than continuing to the right.

Technically, the plane is the universal covering space of the torus. Translations ("shifts"), for example moving trajectories to the left, are deck transformations in the fundamental group $Z \oplus Z$ of the torus. An (m,n)-torus is the $m \times n$-fold covering space of the original torus.

The remainder of the argument relies heavily on the preceeding. If the reader understands the intuition of the preceeding visualization, the remainder of the analysis is straightforward.

The reader is invited to verify that the trajectory of Figure 7 carries the same information as that of Figure 2 (and, indeed, with some folding can be overlaid on it), and that this holds generally. In particular, a (stable) periodic trajectory on the torus corresponds to a (stable) periodic trajectory in the chatterbox.

There is one more bit of notation used below. In the plane the copies $Q_k^{(m,n)}$ touch each other along common edges and, in particular, there are four *corners* of these regions in a fundamental domain. The four *corner corners* are identified to one point—one corner—in the torus. The *lateral corners* on the horizontal and vertical edges of the fundamental domain are respectively identified to two corners, and there is one *central corner* in the middle of the fundamental domain. Each corner is one corner of each of the Q_i in the torus. These corners play a key role in the explication of the dynamics.

There is considerable structure for the dynamics of vector fields on a (2-dimensional) torus, and we exploit this structure. In particular, there is the notion of *rotation number* (see, e.g., [**2**, §11]) which can be defined in a number of ways. Some of the basic properties are:

(a). It is the long-term average slope of any trajectory (one definition).
(b). It is independent of which trajectory, and depends only on the original vector field.
(c). The rotation number depends continuously on the vector field.
(d). There exists a closed periodic trajectory if and only if the rotation number is rational.
(e). Generically, the rotation number is rational with a finite number of resulting periodic trajectories, even in number, alternately stable and unstable.
(f). If the rotation number is irrational, any trajectory is dense, and indeed the flow is topologically conjugate to the flow of a constant vector field with irrational slope (the same irrational).
(g). The non-periodic trajectories are asymptotic to a stable trajectory in positive time and to an unstable trajectory in negative time.

In textbooks, these results are usually proved for continuous vector fields, but the proofs are unchanged for the piecewise constant fields that are relevant for us.

Thus the general theory presents us with the following result, which is a step on the way to Theorem 2.1. Let $\tilde{\Phi}$ denote the set of fields obtained from those in Φ by reorienting.

Lemma 4.1. *There is a generic set of vector fields in* $\tilde{\Phi}$ *with a finite even set of periodic trajectories, alternately stable and unstable. Except for the unstable periodic trajectories, all trajectories asymptote to the stable periodic trajectories.*

What is left is to show that if the number of periodic trajectories is finite, then the number is two—one stable and one unstable.

5. Stability

The next technical step is to develop a formula for determining the stability of periodic trajectories.

Consider a vector field with rational rotation number n/m, where m and n are positive coprime integers. By the general theory of rotation numbers, there is a periodic trajectory P (possibly one of many) of the field. Consider an (m, n)-fold fundamental domain of the torus (as in Figure 7). The trajectory P crosses the lower edge of this (m, n)-fold fundamental domain, say at a point p. Via the dynamics, the trajectory P "moves northeast," through m horizontal fundamental domains and n vertical ones. It hits the right edge of the (m, n)-fold fundamental domain, crossing via a deck transformation to the identified point on the left edge of the (m, n)-fold fundamental domain, and eventually crossing the top edge of the (m, n)-fold fundamental domain at a point q, directly above p, and which is identified with p via a deck transformation, since the trajectory P is periodic. Consider an trajectory P_δ crossing the lower edge at a point p' close to p, say just to the right of p at horizontal distance δ from p. The trajectory P_δ also "moves northeast," eventually crossing the top edge at a point q', say at a distance δ' from q. As $\delta \to 0$, the ratio δ'/δ approaches a positive limit Δ_+. In analogy to smooth differential equations, we call this the *right Floquet number* of P; for the classical Floquet theory, see any basic graduate text in differential equations, e.g., [**4**]. Similarly, a *left Floquet number* Δ_- is defined. If $\Delta_\pm < 1$, orbits nearby to P are closer at the top of the (m, n) fundamantal domain than at the bottom, and thus P is *stable* (from the right or left). Conversely, if $\Delta > 1$, P is *unstable* (from the right or left); if $\Delta = 1$, P is *neutrally stable* (from the right or left) (at least to first order). If P does not pass through any of the corners, then $\Delta_+ = \Delta_-$

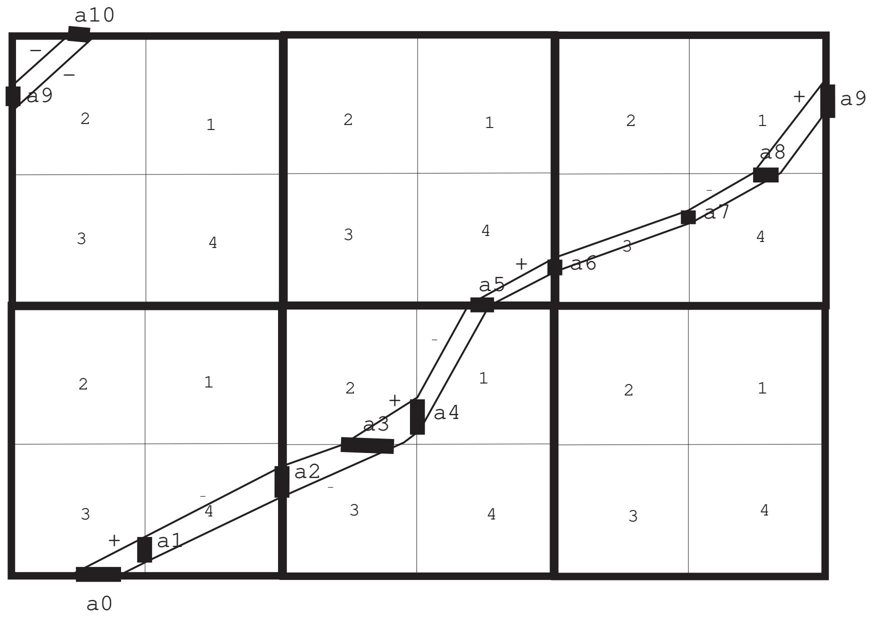

FIGURE 8. Computing stability. The periodic trajectory and a nearby trajectory. The differences $a_0, \ldots, a_{10}$, indicated by heavy bars, are measured. Let $s_1, \ldots, s_4$ be the slopes of the flow in the four quadrants. By similar triangles, $a_1 = s_3 a_0$. This first segment of the trajectory in the third quadrant is labelled + (to indicate the +1 exponent on s_3. Also $a_2 = a_1$, so this trajectory segment is unlabelled (or label "0"). Also $a_3 = s_2^{-1} a_2$, so this segment of the trajectory is labelled "-." The stability is measured by the relation of a_{10} to a_0. It is clear $a_{10} = s_1^{c_1} s_2^{c_2} s_3^{c_3} s_4^{c_4} a_0$ for some integer exponents $c_1, \ldots, c_4$.

and we denote the common value by Δ. This is the most important case, since generically trajectories do not pass through a corner. The logarithm of F is the *Floquet exponent*, which is what is graphed above in Figures 4 and 5.

It is possible to develop an explicit formula for Δ in terms of the original vector fields. Within each Q_i the vector field is constant; denote its slope by s_i.

Lemma 5.1. *Let $\lambda = (s_1 s_3)/(s_2 s_4)$. For any periodic trajectory P which does not pass through a corner, there is an integer d, depending continuously on the trajectory, hence locally constant, such that the Floquet number $\Delta = \lambda^d$.*

Remark. (a). If the trajectory does pass through a corner, there are right and left $d_{\pm}$, which may be (and usually are) different.

(b). The proof is mined for more than the statement of the lemma, in that we determine how d changes as the trajectory is varied.

(c). In Section 6, we prove $d = 0$ or ± 1.

PROOF. Any segment of any trajectory within one of the Q_i is a straight line segment of slope s_i. We suppose our periodic trajectory P does not pass through any corner (if it does, one must make a distinction between trajectories to the right and trajectories to the left of this trajectory). Suppose this segment of the periodic trajectory enters Q_i through the lower edge of Q_i and exits through the right edge. Let δ be so small that the corresponding segment of the nearby trajectory also enters through the lower edge of Q_i and exits through the right edge. Let δx be the horizontal distance between the points of entry of the two trajectories and δy be the vertical distance between the points of exit. Then $|\delta y| = s_i|\delta x|$ (definition of slope). We call such a segment a "+1-segment" (since s_i appears in this formula with exponent $+1$). On the other hand, if the segments enter through the left edge of Q_i at vertical distance δy apart and exit through the upper edge at horizontal distance δx apart, then $|\delta x| = (s_i)^{-1}|\delta y|$, so we call such a segment a "-1-segment," since s_i appears in this formula with exponent -1. If the trajectory segments enter through the lower edge of Q_i and exit through the upper edge of Q_i at distances δx and $\delta' x$ respectively, then $\delta' x = \delta x$. Similarly if the trajectory segments enter through the left edge of Q_i and exit through the right edge of Q_i respectively at distances δy and $\delta' y$ respectively, then $\delta' y = \delta y$. These last two segments we call '0-segments.' If we change notation so that the distance, either horizontal or vertical, between p_j and p'_j is a_j, then $a_{j+1} = s_{i(j)}^{e_j} a_j$, where the jth segment lies in $Q_{i(j)}$, and e_j is 0 or ± 1, depending on the type of segment. This is illustrated in Figure 8.

Let e_i^+ be the number of +1-segments of P in Q_i, let e_i^- be the number of -1-segments, and let $e_i = e_i^+ - e_i^-$. Then, computing segment by segment, we see

$$\Delta = s_1^{e_1} s_2^{e_2} s_3^{e_3} s_4^{e_4}.$$

To complete the proof of Lemma 5.1, we must show

$$e_1 = e_3 = -e_2 = -e_4. \tag{5.1}$$

To this end, we forget that the trajectory comes from a dynamical system and consider only the combinatorics of the trajectory. Fix the (m, n)-fold fundamental domain and the points p and q on the lower and upper edges. We wish to consider

P as a cord that can be contorted into any number of shapes. A *cord* is the union of a sequence of segments w_j $(j = 1, \dots, 4mn)$ of straight lines in the (m, n)-fold fundamental domain with the following properties:

(a). Each straight segment of a cord has positive slope. We consider it as "going" from lower left to upper right;
(b). within any copy of $Q_i^{(j,k)}$ in the (m, n)-fold fundamental domain, the cord is a straight segment, say entering at p_i and exiting at q_i;
(c). no p_i is a corner;
(d). $p_0 = p$, $q_{4mn} = q$, $p_{i+1} = q_i$ for $i = 1, \dots, 4mn - 1$; except
(e). precisely one q_i lies on the right edge of the (m, n)-fold fundamental domain, and p_{i+1} is the point on the left edge of the (m, n)-fold fundamental domain directly to the left of q_i.

Thus in particular, a cord has the same rotation number n/m as the original trajectory. Moreover, the original periodic trajectory P is a cord.

We have no notion of stability for cords which after all, are not trajectories for any relevant dynamics. However, we can speak of $+1$-segments, -1-segments, and 0-segments of cords, can define exponents $e_i^{\pm}$ and e_i for cords, and can consider the validity of equation (5.1).

We next construct a particular cord S as in Figure 9. Without loss of generality, we may suppose that p is in the lower left; i.e., the $(1, 1)$ copy of the fundamental domain in the (m, n)-fold fundamental domain. Let $q_{2n} = p_{2n+1}$ be a point on the lower edge $Q_2^{(1,n)}$ in the upper-left copy of the fundamental domain in the (m, n)-fold fundamental domain, slightly to the right of p. The segment in $Q_2^{(1,n)}$ is a $45°$ segment exiting $Q_2^{(1,n)}$ at $q_{2n+1} = p_{2n+2}$. From this point, the cord S is a straight line sloping slightly upwards until it hits the right edge of the (m, n)-fold fundamental domain at q_{4mn-1}. As required by (e) above, p_{j+1} is on the left edge of the fundamental domain, with the cord S straight from here to q.

Consider the signs of the various segments of S. All segments are 0-segments except two, namely the segment from p_{2n+1} to q_{2n+1} and the segment from p_{4mn} to q_{4mn}, both in the $Q_2^{(1,n)}$. These two segments are respectively a $+1$- segment and a -1-segment. Thus $e_1 = e_2 = e_3 = e_4 = 0$ and equation (5.1) holds.

We next homotope S to the original periodic trajectory P through a sequence of steps; each step preserves equation (5.1). Each step is called "crossing a corner." We indicate the first. In the first step, we alter the three segments from p_{2n} to q_{2n+2}. Originally, these three segments lie in $Q_3^{(1,n)}$, $Q_2^{(1,n)}$, $Q_1^{(1,n)}$. We "lower" these segments, holding p_{2n} and q_{2n+2} fixed, so they lie in $Q_3^{(1,n)}$, $Q_4^{(1,n)}$, $Q_1^{(1,n)}$.

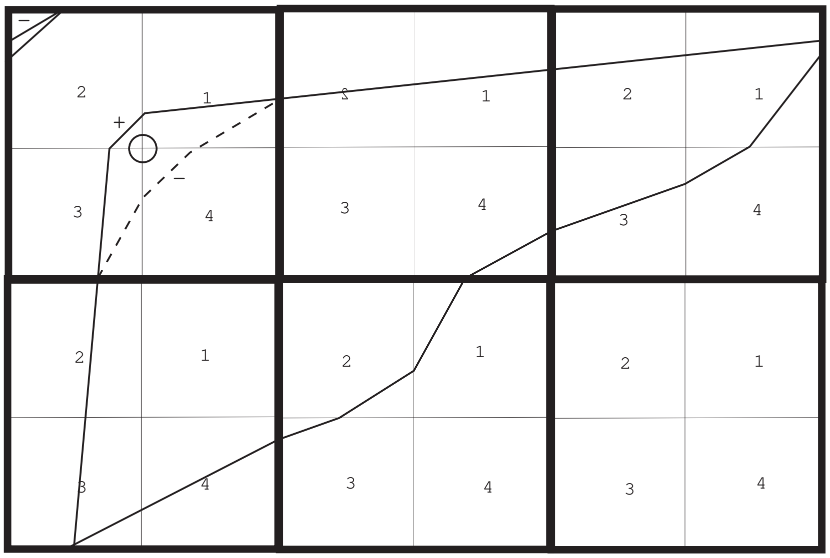

FIGURE 9. The trajectory and a cord S (solid line) and S_1 (dotted line). Note that the cord S has one $+1$-segment and one -1-segment, both in the second quadrant, so that $e_1 = e_2 = e_3 = e_4 = 0$. To deform the cord to the trajectory, as series of moves—lifting the cord across "corners"—are made. Lifting the cord across the circled corner moves this segment of the cord to the dotted line. The effect of this is to replace the $+1$-segment in the second quadrant by a -1-segment in the fourth quadrant; i.e. $e_2 \mapsto e_2 - 1$ and $e_4 \mapsto e_4 - 1$. Also $e_1 \mapsto e_1 + 1$ and $e_3 \mapsto e_3 + 1$. The relations $e_1 = e_3 = -e_2 = -e_4$ are unchanged. Similar calculations follow for other lifts. A finite series of such moves transforms the original cord to the trajectory.

In other words, instead of going to the left and above the center corner in this copy of the fundamental domain, the modified cord S_1 goes below and to the right of the center corner. In this modification, the cord has "crossed this center corner." Both S and S_1 are pictured.

This modified cord S_1 has a new $+1$-segment in the copy of Q_3, a new -1-segment in the copy of Q_4, a new $+1$-segment in the copy of Q_1, and has lost a $+1$-segment in the copy of Q_2. That is, for this modified trajectory, $e_1 = e_3 = 1$, $e_2 = e_4 = -1$, and equation (5.1) remains valid.

It is clear that with a succession of such steps, each crossing just one corner, S can be homotoped to P, and at each step, equation (5.1) remains valid. Thus Lemma 5.1 is proved. □

Remark. We mine the proof for a bit more. Namely equation (5.1) is valid for cords. Moreover, if d is the common value of equation (5.1), we note a step which crosses a center corner or a corner corner changes d by $+1$, and one which crosses a lateral corner changes d by -1.

6. Counting trajectories

The following lemma will complete the proof of Theorem 2.1.

Lemma 6.1. *Suppose a vector field in $\tilde{\Phi}$ has an isolated periodic stable trajectory P and an isolated periodic unstable trajectory P'. Then P and P' are the* only *periodic trajectories of the field.*

Proof. The idea is to consider what happens to the exponents in equation (5.1) as the point p is moved along the lower edge of the (m, n)-fold fundamental domain. We begin with a stable periodic trajectory P that does not pass through any corner, beginning at p and ending at q above p. Suppose p is changed slightly to $\tilde{p} = p + \delta p$. The trajectory $\tilde{P}$ beginning at $\tilde{p}$ is not periodic. The end point of the new trajectory is closer to q than $\tilde{p}$ is to p. We alter the new trajectory slightly to a (periodic) cord by changing its last segment, originally from $\tilde{p}_{4mn}$ to $\tilde{q}_{4mn}$. Let $\tilde{q}$ be the point on the upper edge of the (m, n)-fold fundamental domain directly above $\tilde{p}$, and change the last segment so it goes from $\tilde{p}_{4mn}$ to $\tilde{q}$ instead of $\tilde{q}_{4mn}$. It is now a cord $\tilde{S} = \tilde{S}_{\tilde{p}}$ from $\tilde{p}$ to $\tilde{q}$ and we can consider the exponents e_i (it may be necessary to slightly modify the first condition in the definition of cords in that the last segment may have infinite or negative slope; however this does not affect the combinatorics).

We consider the exponent d as a function $d_{\tilde{p}}$ of $\tilde{p}$. If δp is small enough that none of the cords between P and $\tilde{S}_{\tilde{p}}$ pass through a corner, the exponents e_i are the same for $\tilde{S}_{\tilde{p}}$ as for P, and in particular, $d_{\tilde{p}}$ does not change. That is, $d_{\tilde{p}}$ changes only when the cord $S_{\tilde{p}}$ passes through a corner. From the argument of Section 5 we know that, when the trajectory passes through a single corner, $d_{\tilde{p}}$ changes by ± 1. We may assume that the cords do not pass through more than one corner, for if so, we may slightly modify the cords so this does not happen.

We next consider copies of P in the (m, n)-torus. In the (m, n)-torus, there are mn copies of p (in the (m, n)-fundamental domain those on the right or upper edges are duplicates and do not count), namely one each in each copy of the mn

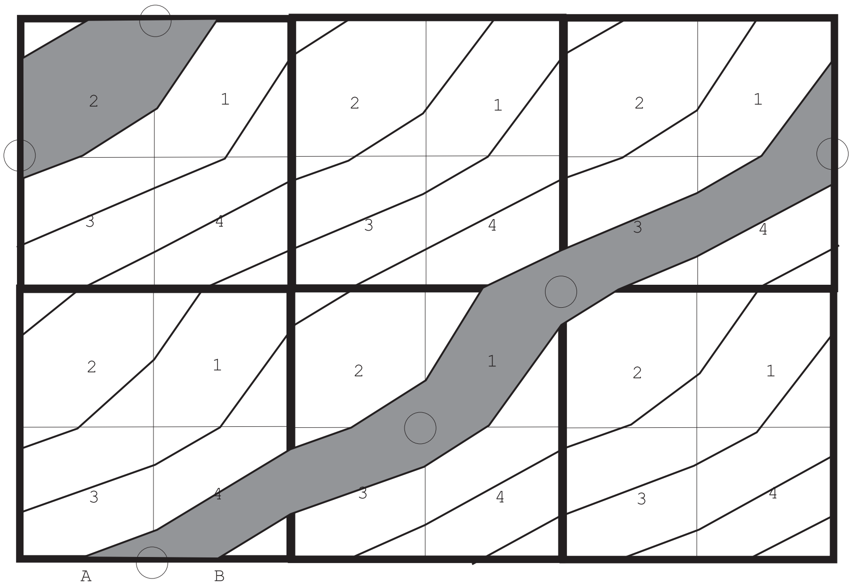

FIGURE 10. The trajectory and the $n \cdot m$ ($= 3 \cdot 2$ in this case) copies of it in the $n \times m$-fold cover of the fundamental domain, and a shaded copy of one of the $n \cdot m$ congruent regions between. Since there are $4n \cdot m$ corners in the $n \times m$ cover, each of the congruent regions contains exactly 4 corners. The corners in the shaded region are indicated by circles—the two circled corners in the upper left portion of the shaded region are shifts of corners in the other portion. As the initial point of the trajectory varies from "A" to "B," the resulting trajectories, modified as indicated in the text to closed strings, covers the shaded region and hence crosses exactly four corners.

copies of the fundamental domain. Through each of these passes a copy of the periodic trajectory P. That is, there are mn copies of P in the (m, n)-torus. The regions between these copies are congruent (since they are translates of each other by deck transformations of the fundamental group of the basic torus). Since there are a total of $4mn$ corners in this torus, each inter-trajectory region contains *exactly* four corners. This is illustrated in Figure 10.

As δp increases so that $\tilde{p}$ moves to the right of p, it is clear that $\tilde{p}$ eventually returns to a copy of P. In fact, by the previous paragraph, during this sojourn of $\tilde{p}$,

$d_{\tilde{p}} \longrightarrow$				
At P	After 1 corner	After 2 corners	After 3 corners	After 4 corners
k	$k+1$	$k+2$	$k+1$	k
k	$k+1$	k	$k+1$	k
k	$k+1$	k	$k-1$	k
k	$k-1$	k	$k+1$	k
k	$k-1$	k	$k-1$	k
k	$k-1$	$k-2$	$k-1$	k

TABLE 2. Values of d during sojourn of $\tilde{p}$. One considers a stable periodic trajectory P and considers the effect of on the index of moving P to the right, reading from left to right. We assume $\lambda < 0$ so $k > 0$. Each time this moving P crosses a corner, d changes by ± 1. Thus each vertical line in the table corresponds to crossing a corner. After four crossings, the trajectory has returned to P and the final value of d is the same as the initial value. There are six possible ways for these changes in the index to occur, listed in the six rows. Only the last one (with $k = 1$) yields both stable and unstable trajectories.

precisely four corners are crossed. Also during this sojourn, an unstable periodic trajectory P' is reached. Recall that there are a finite number of discrete periodic trajectories, alternately stable and unstable. Generically $\lambda = (s_1 s_3)/(s_2 s_4) \neq 1$; suppose for definiteness that $\lambda < 1$. Then a periodic trajectory is stable if and only if $d_{\tilde{p}} > 0$, say $d_{\tilde{p}} = k$. There must also be an unstable periodic trajectory P' with $d_{\tilde{p}'} < 0$. During the sojourn, $d_{\tilde{p}}$ changes four times, ending at the same value of $d_{\tilde{p}}$, so there are six possibilities, as given in Table 2. Recall (remark at end of Section 5), that each change of $d_{\tilde{p}}$ is by ± 1. Only one possibility yields both a positive and a negative value of $d_{\tilde{p}}$, namely the last possibility in the table, and moreover it must be that $k = 1$. Within a region where $d_{\tilde{p}} > 0$, there can be at most one periodic trajectory, and similarly within a region where $d_{\tilde{p}} < 0$, there can be at most one unstable periodic trajectory. Thus there is precisely one of each. Lemma 6.1 and Theorem 2.1 are proved. $\square$

7. Other proofs

In this section, we prove Theorems 2.2 and 2.3.

Proof. (Theorem 2.2.) We prove that whenever the Filippov coefficients c_i are well-defined, the vector (2.6) is in R^{d-2}. That is, the total flow has no transversal component, equivalently the frozen flow averaged over time is zero. In our case, generically there is a single stable periodic trajectory P. This periodic trajectory consists of segments of straight lines, indexed say by i. The flow moves with velocity v_i along each segment and spends time t_i on it. The Filippov condition states that

$$\sum_i t_i v_i = 0.$$

Note that $t_i v_i$ is the directed length of the segment i, so the sum is the sum of the directed lengths. Since the trajectory is periodic, the sum of the directed lengths is zero, and the Filippov condition is verified. □

Proof. (Theorem 2.3.) At this point, Theorem 2.3 follows from general theory. The set of vector fields $f_i(x,y,z)$ on B satisfying the conditions of Section 2 form a locally compact metric space $\hat{\Phi}$, under the topology of uniform convergence, as do the reflected vector fields $\hat{\hat{\Phi}}$. By the general theory of flows of doubly-periodic vector fields, there is a generic set $\hat{\hat{\Phi}}'$ of doubly-periodic fields with the properties of Lemma 4.1. In particular, any field $\phi \in \hat{\hat{\Phi}}'$ has a neighborhood of fields $\phi' \in \hat{\hat{\Phi}}'$ such that the periodic orbits of ϕ' approximate those of ϕ. In particular, the amount of time a periodic trajectory of ϕ' spends in any reasonable set (in particular any Q_j) approximates the amount of time the corresponding periodic trajectory of ϕ. In our context, there is only one stable periodic trajectory, and hence, (2.7) holds. Thus Theorem 2.3 is established. □

8. Discussion

With the notation and concepts of Sections 5 and 6, we revisit the behavior of the dynamics, as pictured in Figure 7. Within an interval of the parameter τ where the rotation number is constant, genericity obtains and there is a unique stable periodic trajectory P_τ which does not pass through any corners. The stable periodic trajectory P_τ depends continuously on the parameter and the c_i are continuous. Except for a single unstable periodic trajectory, all trajectories asymptote to P_τ in positive time. At the ends of such a parameter interval, the P_τ passes through a corner. At these parameter values P_τ has different left and right Floquet numbers; the trajectory is stable on one side and neutrally stable on the other. At this τ, there is indeed a continuum of neutrally stable periodic trajectories on the neutrally stable side of P_τ. These trajectories are all identical in shape and length; they are translates of each other. These trajectories have different c_i, and the concept of well-defined c_i breaks down.

As the parameter value is varied beyond the end of one of these intervals of constant rotation number (m, n), the dynamics change rapidly and the rotation number varies, but continuously. As the continuum of neutrally stable periodic trajectories is perturbed, trajectories of irrational rotation number occur—these are not periodic—and periodic trajectories of rotation number (m', n') with $m' > m$ and $n' > n$ appear. The graph of the rotation number takes on the standard form of a "devil's staircase."

As discussed at the beginning of the paper, the investigations in this paper are for "frozen" dynamics. For the application, there is a slow (in the present time scale) motion along the sliding surface, which results in a change in the transversal vector field. In particular, although generically a single stable periodic trajectory obtains, the motion along the sliding surface likely will take the transversal dynamics through non-generic states. At these states, our analysis breaks down, and a description of the behavior of the dynamics is not possible without a further refinement of the model of the underlying mechanism.

The arguments of the paper yield a refinement for the algorithm for numerically locating the stable periodic orbit, and hence the Filippov coefficients $c_i(z)$. For a generic field (one with a stable orbit), a generic orbit converges to the stable periodic orbit. Suppose such a generic orbit has been run long enough that it is sufficiently close (which means the process below works) to the stable orbit. In particular, the appropriate (m, n) is apparent. For a small horizontal interval at the bottom of the (m, n)-torus (as in Figure 7), the map that takes any point on this interval via the dynamics to a point at the top of the (m, n)-torus is affine, since it is the composition of a sequence of affine maps in each $Q_{(i,j)}$. That is, it has the form $x \mapsto Ax + B$. Moreover, since one orbit has been computed, the value of this map at (at least) one x is known. Furthermore, A is nothing but the Floquet number, which is computed from the slopes of the vectors. Thus we know the map (the "point-slope" formula), and hence can compute its fixed point, which is the x-value of the stable orbit.

Finally, we note the analysis depends critically on properties of 2-dimensional dynamics, so the methods, and almost certainly the results, do not extend to higher multiples of intersections.

References

1. J. C. Alexander and T. I. Seidman, *Sliding modes in intersecting switching surfaces I: Blending*, Houston J. Math. (1998), in press.

2. V. I. Arnold, *Geometrical Methods in the Theory of Ordinary Differential Equations*, Grundlehren der mathematischen Wissenschaften, no. 250, Springer-Verlag, Berlin, 1983.

3. A. F. Filippov, *Differential Equations with Discontinuous Righthand Sides*, Kluwer, Dordrecht, 1988.

4. P. Hartman, *Ordinary Differential Equations*, Birkhauser, Boston, 1982.

5. T. I. Seidman, *Some limit problems for relays*, in Proceedings of the First World Congress of Nonlinear Analysts, V. Lakshmikantha, ed., vol. I, Walter de Gruyter, Berlin, 1995, 787–796.

6. V. I. Utkin, *Sliding Modes in Control and Optimization*, Communications and Control Engineering Series, Springer-Verlag, Berlin, 1992.

Department of Mathematics, University of Maryland, College Park, MD 20742-4015, USA

E-mail address: jca@math.umd.edu

Department of Mathematics and Statistics, University of Maryland, Baltimore County, Baltimore, MD 21250, USA

E-mail address: seidman@math.umbc.edu